T cell-secreted TNF-alpha induces emergency myelopoiesis and myeloid-derived suppressor cell differentiation in cancer

Mohamad F. Al Sayed, [1,2,*] Michael A. Amrein, [1,2,*] Elias D. Bührer, [1,2] Anne-Laure Huguenin, [1,2] Ramin Radpour, [1,2] Carsten Riether, [1,2] and Adrian F. Ochsenbein, [1,2,†]

[1]Tumor Immunology, Department of BioMedical Research, University of Bern, Switzerland.

[2]Department of Medical Oncology, Inselspital, Bern University Hospital, University of Bern, Switzerland

[*] Equally contributing

†Correspondence: Department of Medical Oncology, Inselspital, Bern University Hospital and University of Bern, 3010 Bern, Switzerland; e-mail: adrian.ochsenbein@insel.ch

Running Title: T cell-secreted TNF-alpha activates myelopoiesis in cancer

Article main text count: 5344

Abstract word count: 159

Figures: 7

References: 58

Keypoint: T cell-secreted TNFα activates emergency myelopoiesis in cancer

Abstract

Hematopoiesis in cancer patients is characterized by reduced production of red blood cells and an increase in myelopoiesis, which contributes to the immune-suppressive environment in cancer. Some tumors produce growth factors that directly stimulate myelopoiesis such as G-CSF or GM-CSF. However, for a majority of tumors that do not directly secrete hematopoietic growth factors, the mechanisms involved in the activation of myelopoiesis are poorly characterized. In this study, we document in different murine tumor models activated hematopoiesis with increased proliferation of long-term and short-term hematopoietic stem cells and myeloid progenitor cells. As a consequence, the frequency of myeloid-derived suppressor cells (MDSC) and its ratio to $CD8^+$ T cells increased in tumor-bearing mice. Activation of hematopoiesis and myeloid differentiation in tumor-bearing mice was induced by tumor necrosis factor alpha (TNF-α), which was mainly secreted by activated $CD4^+$ T cells. Therefore, the activated adaptive immune system in cancer induces emergency myelopoiesis and immunosuppression.

Introduction

Steady-state hematopoiesis in the BM is a tightly controlled and regulated process that ensures the continuous generation of all blood lineages (1). In cancer, hematopoiesis is perturbed and characterised by a preferential myeloid differentiation at the expense of erythroid and lymphoid differentiation (2). This leads to the accumulation of immature and immunosuppressive myeloid cells, primarily myeloid-derived suppressor cells (MDSCs) (3,4). In mice, MDSCs express granulocytic ($CD11b^{+}Ly6G^{+}Ly6C^{lo}$; Gr-MDSC) or monocytic markers ($CD11b^{+}Ly6C^{+}Ly6G^{lo}$; M-MDSC) (5). They suppress the adaptive immune response to cancer and promote tumor growth by promoting tumor cell survival, angiogenesis and metastasis (4,5). MDSCs are short-lived and have to be continuously replenished from hematopoietic stem and progenitor cells (HSPCs) in the BM and with subsequent mobilization and acquisition of immunosuppressive activity in the tumor microenvironment (5). Although the mechanisms are not yet fully understood, the accumulation of MDSCs and the aberrant myelopoiesis in cancer patients are attributed to the secretion of tumor-derived factors. Hematopoietic cytokines such as GM-CSF, G-CSF, IL-6 and IL-1 are produced in variety of human tumors such as brain, colorectal and lung cancer and regulate the production of MDSCs from BM progenitors (6-8). In the MMTV-PγMT breast cancer mouse model, G-CSF released by mammary tumor cells induced hematopoietic stem cell (HSC) expansion and granulopoiesis in the BM to replenish short-living MDSCs (7,9). Similarly, it has been documented that tumor growth in Lewis lung carcinoma model is accompanied with an increase in peripheral myeloid cells and $lin^{-}c\text{-}kit^{+}sca\text{-}1^{+}$ stem and progenitor cells (LSKs). This was attributed to Insulin-like growth factor-I receptor (IGF-IR) signaling in HSCs (10). Furthermore, GM-CSF has been shown to induce the differentiation of granulocyte-monocyte-myeloid progenitors (GMPs) at the expense of lymphoid and erythroid progenitors (11). Similarly, GM-CSF-secreted by mammary 4T1 tumors led to the expansion of myeloid progenitors and accumulation of $CD11b^{+}GR\text{-}1^{+}$ myeloid cells (12). In addition, TNFα has been shown to lead to the accumulation of MDSCs in murine and human tumors (13,14).

Importantly, the vast majority of solid tumors do not secrete hematopoietic cytokines (8). The mechanisms underlying the modulation of myelopoiesis in these tumors are poorly understood. In this study we document an activated hematopoiesis with increased numbers of long-term (LT) and short-term (ST) HSCs and myeloid progenitor cells in transplanted, chemically-induced and spontaneous murine tumor models. This led to an accumulation of immunosuppressive MDSCs in tumor-bearing mice. Interestingly, TNFα secreted by T cells induced proliferation of HSPCs, myeloid differentiation and the accumulation of MDSCs. Therefore, the activated adaptive immune system in cancer induces immunosuppressive myeloid cells that dampen the tumor-specific immune response.

Materials and Methods

Mice

C57BL/6 (BL/6), Rag-1$^{-/-}$ (Rag$^{-/-}$), IFNγ-R$^{-/-}$, TNFR1/2$^{-/-}$ and Ly5.1 mice were from the Institute of Laboratory Animal Science (Zurich, Switzerland). IL-6$^{-/-}$ mice were obtained from M. Kopf (Swiss Federal Institute of Technology). Ubi-GFP mice were from C. Müller (Institute of Pathology, University of Bern). *K-ras*$^{LSL-G12D/WT}$*; p53*$^{Flx/Fx}$ (KP) mice were kindly provided by Alfred Zippelius, Tumor Immunology, University of Basel. All animals were on BL/6 background. All animal experiments were performed in 6 to 8 weeks old mice, housed in a specific pathogen-free facility. All animal experiments were approved by the Veterinary Office of the Canton Bern and performed according to Swiss laws for animal protection.

Tumor models

MC57, MC38, B16F10 and 3LL tumors were induced as described in Matter et al (15). Briefly, tumor single cell suspensions were injected subcutaneously (s.c.) into the flanks of Rag$^{-/-}$ mice. After 14 days, tumors were collected and non-necrotic tissue was cut into small fragments (1-2mm^3). Tumor fragments were then transplanted s.c. in the flanks of recipient mice. Tumor volume was calculated according to the formula $V=\pi \times abc / 6$, where *a*, *b*, and *c* are orthogonal diameters**.** For methylcholanthrene (MCA)-induced tumors, 250ug of MCA dissolved in sunflower oil was injected s.c. into shaved flanks of BL/6 mice (control: sunflower oil). For tumor induction in KP transgenic mice, an adenoviral vector expressing Cre recombinase was intratracheally injected into six-week-old KP mice. (16).

Cell lines

MC57 fibrosarcoma, B16F10 melanoma, MC38 colon adenocarcinoma and mouse Lewis lung carcinoma 3LL cell lines were a gift from Prof. Rolf Zinkernagel, Institute of experimental immunology, University of Zurich (Zurich, Switzerland) and have been characterized and described before (15,17). No additional authentication was performed. Cell cultures were regularly tested for mycoplasma contamination.

BM lineage depletion

BM lineage depletion was performed by magnetic-activated cell sorting (MACS) negative selection using biotinylated Abs against red blood cell precursors (α-Ter119), B cells (α-CD19), T cells (α-CD3ε), and myeloid cells (α-Gr1), MACS α-biotin beads, and LS columns (Miltenyi Biotec). Negative cell fraction was used for analysis or further cell sorting.

Antibodies and Flow cytometry

Anti-mouse mAbs against the following antigens were used for flow cytometry: CD4 (GK1.5), CD8 (53-6.7), CD3ε (145-2C11), CD19 (6D5), CD11b (M170), Ly6C (HK1.4), Ly6G (1A8), Gr1 (Ly6C/G; RB6-8C5), c-kit (2B8), CD34 (RAM34), CD16/32 (FcγR; 93), IL-7Rα (CD127; A7R34), CD90.1 (Ox-7), CD90.2 (30-H12), CD48 (HM48-1), CD135 (A2F10), CD150 (TC15-12F12.2), CD45 (30-F11); Sca-1 (D7), CD45.1 (A20), CD45.2 (104) and BrdU and isotype (BD Pharmingen). Cells were washed in PBS and resuspended in the corresponding fluorescence-activated cell sorting (FACS) antibodies for 30 minutes at 4°C. Cells were then washed in PBS and analyzed on a LSRII (BD Biosciences). Alternatively, cells of interest were FACS-sorted by FACS Aria II (BD Biosciences). Data were analyzed with FlowJo software (Treestar, Ashland, OR).

Blood analysis

Blood was collected into EDTA-coated tubes and white blood cell counts were determined using a Vet ABC animal blood counter (Medical Solution GmbH) and/or by FACS staining.

Isolation of tumor-infiltrating lymphocytes (TILs)

Tumors were cut into very small pieces by a scalpel, digested for one hour at 37°C in PBS supplemented with 1 mg/mL Collagenase-IA, 100 μg/mL Hyaluronidase-V (Sigma), 40 U/mL DNase-I (Roche), 5 mmol/L $CaCl_2$, and 5 mmol/L $MgCl_2$, washed and filtered to get a single cell suspension. TILs were

isolated by positive magnetic cell sorting (MACS) of $CD45^+$ cells using biotinylated-anti-CD45, MACS anti-biotin beads and LS columns (Miltenyi Biotec).

Colony forming assays

FACS-sorted HSPCs, Lin^- BM cells, splenocytes or blood cells were plated into MethoCult M3134 medium (STEMCELL Technologies) supplemented with 15% FCS, 20% BIT (50 mg/ml BSA in IMDM, 1.44 U/ml rh-insulin [Actrapid; Novo Nordisk], and 250 ng/ml human holo transferrin [Prospec]), 100 µM 2-mercaptoethanol, 100 U/ml penicillin, 100 µg/ml streptomycin, 2 mM L-glutamine, and 50 ng/ml rm-SCF, 10 ng/ml rm-IL-3, 10 ng/ml rh-IL-6, and 50 ng/ml rm-Flt3-ligand (Prospec). Colonies were counted after 7 days on a DMIL inverted microscope (Leica) equipped with an Intensilight C-HGFI unit (Nikon). For some assays, cells were incubated overnight with 10% sera, T cell-conditioned media or tumor cell line-conditioned media before applying to the colony one day later. 5 ug/ml blocking antibodies for IL-6 (clone MP5-20F3; Biolegend), TNFα (clone MP6-XT22, Biolegend) or CCL3 (clone 39624; R&D) were added to the overnight cell culture where indicated. Control colonies were supplemented with the corresponding isotype controls.

Cell cycle analysis

C-kit^{hi}, LSKs, CMPs and GMPs were sorted by BD FACS Aria (BD) sorter and incubated in 1% PFA/PBS overnight at 4°C. Samples were permeabilized with 0.2% Triton X-100 for 30 min at 4°C and labeled with 5 µg/ml DAPI (Roche).

T cell suppression assay

FACS-sorted $CD11b^+Gr1^+$ MDSCs from tumor-bearing or naive mice were cultured with anti-CD3ε-stimulated T cells from BL/6 mice in a ratio of 3:1, for 3 days. [^{3}H]-Thymidine was added to the culture during the last 16 hours of stimulation. [^{3}H]-Thymidine incorporation was measured using a scintillation beta counter.

BrdU incorporation *in vivo*

Animals were treated with BrdU (Sigma; 0.8 mg/mL in drinking water and 1 mg intraperitoneally (i.p.) /d) on 2 consecutive days and BrdU staining was performed as described in the manufacturer's instructions (BrdU Flow kit; BD).

BM transplantation

Recipient mice were lethally irradiated (2× 6.5 Gy within a 4-hour interval) with a Gamma cell 40 (MDS Nordion). Whole BM cells or $CD45^+$ cell from tumors (10^5 cells) were transplanted along with congenic competitor BM cells ($2x10^5$ cells) at ratios of 1:2 into recipient mice. During 1-2 weeks after transplantation, antibiotics were added to the drinking water.

T cell depletion and neutralization of TNFα *in vivo*

For T-cell depletion mice were treated i.p. on day -1, day 0 and then every week after tumor transplantation with 100 μg anti-CD4 antibody (clone GK1.5; BioXcell) or anti-CD8 (clone YTS 169.4; BioXcell) antibody or both, together with the appropriate isotype control from rat serum. T cell depletion in blood was controlled by FACS prior to tumor transplantation. Depleting efficiency was higher than 98%. TNFα was neutralized in vivo by administration of anti-TNFα (clone XT3.11; BioXcell) or isotype control (clone BE0290; BioXcell) twice a week starting at the time point of tumor transplantation.

T cell conditioned media (TCM)

$CD4^+$ or $CD8^+$ T cells were sorted by FACS from spleens of naive or tumor-bearing mice 30 days after tumor transplantation. $3.5x10^5$ cells/well were incubated in RPMI 10% FCS for 16 hours at 37°C 5% CO_2. Supernatants were then collected after centrifugation.

Cytokine analysis

48 mouse cytokines, chemokines and growth factors were analyzed in sera or TCM using the Multiplexing LASER Bead Assay (Eve Technologies): IL-1α, IL-12 (p70), IL-33, RANTES, IL-1β, IL-13, Eotaxin, M-CSF, IL-2, IL-15, IP-10, G-CSF, IL-3, IL-17A, KC, GM-CSF, IL-4, IL-17F, LIF, IFNγ, IL-5, IL-17E/IL-25, LIX, TNFα, IL-6, IL-21, MCP-1, TNFβ, IL-7, IL-22, MIG, TGF-β1, IL-9, IL-23, MIP-1α, TGF-β2, IL-9, IL-27, MIP-1β, TGF-β3, IL-10, IL-28B, MIP-2, VEGF, IL-12 (p40), IL-31, MIP-3α, CD40L. GM-CSF was measured in conditioned media of different tumor cell lines. Heatmaps were generated using standard Ward's method according to the standard normal distribution.

Cell signaling and *in silico* pathway analysis

Canonical pathway representing differentially expressed cytokines were identified using the Ariadne Genomics Pathway Studio® software, version 9 (Elsevier). The data set containing protein (cytokine) names and corresponding fold changes were uploaded into the Pathway Studio. The analysis identified the direct interactions between TNFα and other differentially expressed cytokines.

Statistical analysis

Statistical analysis was performed using GraphPad Prism 5.0 (GraphPad Software). Data are represented as mean ± SEM. The Shapiro-Wilk test was used to determine whether the data meet the assumption of normality. Data were analyzed using 1-way ANOVA and Tukey's multiple comparison test, Student's *t* test (2-tailed), 1-sample *t* test or 2-way ANOVA, and Bonferroni's post-hoc test (*P* value shows interaction). $*P < 0.05$ was considered significant, $**P < 0.01$, and $***P < 0.001$.

Results

Increased numbers of myeloid cells in spleen and BM of tumor-bearing mice

In order to study the mechanisms how solid tumors influence hematopoiesis, we transplanted solid fragments of the fibrosarcoma MC57 subcutaneously (s.c.) to BL/6 mice (15). Recipient mice developed clinically detectable tumors after approximately 1 week that grew up to $1cm^3$ within 4 weeks after transplantation (Supplementary Fig. S1A). The analysis of white blood cells in the circulation and in BM revealed an increase in myeloid cells and a decrease in T cell numbers (Supplementary Fig. S1B-D). Larger tumors often develop a central necrosis. This may explain the lack of increase of leukocytes and granulocytes at the end of the experiment. Similarly, frequencies of T and B cells in spleen were reduced whereas the frequency of myeloid $CD11b^+$ cells was increased in tumor-bearing mice (Fig. 1A). $CD11b^+Gr1^+$ MDSC numbers were significantly increased in spleen and BM of tumor-bearing mice compared to naive mice (Fig. 1B). Importantly, the ratio of T cells to MDSCs was significantly reduced in tumor-bearing mice (Fig. 1C). The number of MDSCs in spleen, BM and in the tumor correlated with the tumor size (Fig. 1D). To test MDSCs functionally *in vitro*, we stimulated T cells from BL/6 naive mice with anti-CD3ε antibody in the presence of FACS-sorted $CD11b^+Gr1^+$ MDSCs from naive or tumor-bearing mice. Proliferation of activated T cells, assessed by [^{3}H]-thymidine incorporation, was significantly lower in the presence of MDSCs from tumor-bearing mice compared to controls (Fig. 1E). This data indicates that hematopoiesis in tumor-bearing mice is skewed towards a preferential accumulation of immunosuppressive myeloid cells.

Hematopoietic stem and myeloid progenitor cells increase in numbers in tumor-bearing mice.

The increase in myeloid cells in tumor-bearing mice depends on an accelerated myelopoiesis in the BM. We therefore performed a detailed analysis of HSPCs in the BM of tumor-bearing mice and naive controls. The number of lineage-negative (Lin^-) HSPCs was significantly higher in tumor-bearing mice than in controls (Fig. 2A). Similarly, numbers of LSKs, Lin^- $sca\text{-}1^-$ $c\text{-}kit^+$ $CD34^+$ $Fc\gamma R^-$ common myeloid

progenitors (CMPs) and Lin$^-$ sca-1$^-$ c-kit$^+$ CD34$^+$ FcγR$^+$ GMPs were elevated in tumor-bearing mice (Fig. 2B). However, numbers of Lin$^-$ c-kit$^+$ CD127$^+$ CD90.1/2$^-$ common lymphoid progenitors (CLPs) were comparable (Fig. 2C). In addition, FACS-purified Lin$^-$ cells, LSKs and CMPs from the BM of tumor-bearing mice formed more colonies in methylcellulose than the respective cell populations from control mice (Fig. 2D). A phenotypical subdivision of the LSK population revealed higher numbers of long-term HSCs (LT-HSC, CD34$^-$CD48$^-$CD135$^-$CD150$^+$), short- term HSCs (ST-HSC, CD34$^+$CD48$^-$CD135$^-$ CD150$^+$) and the multipotent progenitors (MPP1, CD34$^+$CD48$^+$CD135$^-$CD150$^+$ and MPP2, CD34$^+$CD48$^+$CD135$^-$CD150$^-$) in tumor-bearing mice (Fig. 2E). In contrast, numbers of MPP3 (CD34$^+$CD48$^+$CD135$^+$CD150$^-$) that are known to be skewed towards lymphoid differentiation (18) remained constant (Fig. 2F). This is in agreement with our observation of comparable numbers of CLPs in both tumor-bearing and naive mice (Fig. 2C).

Inflammatory stimuli activate and mobilize HSPCs into the circulation and to extramedullary tissues (19,20). Numbers of Lin$^-$ cells increased significantly in the spleen and blood of tumor-bearing animals (Fig. 2G). The increased number of HSPCs in spleen and blood was confirmed functionally by colony-forming assays (Fig. 2H). In addition, LSKs were detected in the tumor tissue (Fig. 2I). Importantly, isolated LSKs from tumors were functional and reconstituted hematopoiesis in lethally irradiated recipient mice similar to BM LSKs isolated from naive mice (Fig. 2J). In summary, hematopoiesis in tumor-bearing mice is activated with increased mobilization and myeloid differentiation.

HSPCs from tumor-bearing mice are increased in numbers and exhibit higher cycling activity.

To determine whether the elevated numbers of HSPCs are due to enhanced proliferation, we performed a cell cycle analysis of HSPCs using DAPI staining. C-kit^{hi} HSPCs, LSKs and CMPs from tumor mice showed a higher frequency of cells in the replicating S-phase and a lower fraction in the G1-phase of the cell cycle (Fig. 3A and Supplementary Tab. S1). GMPs showed a similar trend, however to a lesser extent. In addition, a higher BrdU incorporation *in vivo* in LSKs and CMPs and a trend to a higher incorporation in GMPs, confirmed an enhanced proliferation of HSPCs in tumor-bearing mice (Fig. 3B and

Supplementary Tab. S2). In contrast, there were no significant changes in Annexin-V^+ cells for CMPs, GMPs and LSKs in tumor-bearing or naive mice (Fig. 3C and Supplementary Tab. S2).

To functionally validate the findings of increased numbers of HSPC in tumor-bearing mice, we transplanted BM cells (Ly5.2) into lethally irradiated Ly5.1 recipient mice (Fig. 3D). In line with our previous results, BM cells from tumor-bearing mice reconstituted primary recipient mice more efficiently compared to BM cells from naïve mice. This was demonstrated by higher percentage of donor $Ly5.2^+$ total cells and LSKs in Ly5.1 recipients of BM cells from tumor-bearing rather than naïve mice (Fig. 3E-F). These results functionally confirm a higher number of HSPC in tumor-bearing mice.

Activation of HSCPs depends on the tumor model.

We next tested whether the observed changes in myelopoiesis are limited to MC57 fibrosarcoma or if other tumors can similarly activate HSPCs. To this end, we analyzed HSCPs in different murine tumor models. Tumor-bearing mice with MC38 colon carcinoma and B16F10 melanoma did not show significant alterations in the numbers of HSPCs in the BM. Moreover, *in vitro* assays revealed a comparable colony forming capacity of HSPCs from tumor-bearing or naive mice (Fig. 4A-D; Supplementary Fig. S2A-B and Supplementary Tab. S3). In contrast, LSKs and GMPs were increased in mice with 3LL Lewis lung carcinoma (Fig. 4E; Supplementary Tab. S3 and Supplementary Fig. S2C) and HSPCs from tumor mice formed more colonies compared to naive mice (Fig. 4F).

To mimic a more physiological situation of tumor development, we inoculated MCA into the flank of BL/6 mice. Mice that developed chemically-induced tumors had higher numbers of LSKs and slightly higher numbers of CMPs in BM (Fig. 4G and Supplementary Tab. S3). This was accompanied by a higher colony formation capacity *in vitro* (Figure 4H). Finally, we analyzed BM HSPCs in a genetically engineered mouse model of lung adenocarcinoma. In this model, tumor formation is driven by a conditional overexpression of *K-ras*^{G12D} in combination with loss of *p53* (*K-ras*$^{LSL\text{-}G12D/WT}$*; p53*$^{Flx/Flx}$ (KP)) (16). KP mice developed autochthonous lung tumors after inhalation of adenoviral vectors expressing Cre recombinase. Tumor-bearing mice had significantly higher numbers of c-kit^{hi} cells, LSKs, CMPs and

GMPs and HSPCs formed more colonies *in vitro* compared to non-tumor bearing littermate mice (Fig. 4I-J and Supplementary Tab. S3). Therefore, HSPC numbers and myelopoiesis are increased in several, but not all tumor models.

HSPCs and myelopoiesis are activated by the adaptive immune system in tumor-bearing mice.

Tumors can activate hematopoiesis through the secretion of various cytokines such as GM-CSF and other CSFs (7,21-23). However, tumor-conditioned media did not significantly enhance colony formation of LSK (Fig. 5A). In addition, GM-CSF concentrations were not detectable in cultures, except for MC38-conditioned medium (Fig. 5B). Interestingly, although MC38 cells produced detectable levels of GM-CSF, this was not sufficient to activate myelopoiesis *in vivo* (Fig. 4A).

Alternatively, the inflammatory environment induced by the tumor may indirectly influence HSPCs in the BM. Interestingly, HSPC numbers were increased in tumors that are known to be immunogenic (MC57, 3LL, MCA-induced tumors and KP lung tumors (24-28)). In contrast, HSPCs remained unchanged in low to non-immunogenic tumors such as MC38 and B16F10 (29,30). To investigate a potential role of the adaptive immune system in the activation of HSPC compartment, we transplanted MC57-tumor fragments to $Rag^{-/-}$ mice that lack mature T, B and NKT cells (31). In the absence of the adaptive immune system, numbers of HSPCs and the colony formation capacity did not increase in tumor-bearing mice (Fig. 5C, D). In addition, MDSC numbers in tumor-bearing $Rag^{-/-}$ mice increased significantly less than in tumor-bearing BL/6 mice (Fig. 5E). These experiments indicate that myelopoiesis in tumor-bearing mice was increased by the adaptive immune system.

Increased myelopoiesis in tumor-bearing mice depends on soluble factors secreted by activated T cells.

To confirm the results observed in the $Rag^{-/-}$ mice and to analyze which cell population of the adaptive immune system is responsible for the activation of HSPCs, we depleted $CD4^+$, $CD8^+$ or both T cell populations before MC57 tumor transplantation in BL/6 mice. Depleting $CD4^+$ and $CD8^+$ T cells in naive

mice did not change LSK numbers in the BM (Fig. 6A). In contrast, depletion of $CD4^+$ and $CD8^+$ T cells normalized LSKs and CMPs numbers. Single depletion of $CD4^+$ T cells similarly normalized HSPC numbers, whereas depletion of $CD8^+$ T cells alone did not (Fig. 6A). In addition, we analyzed the effect of T cell depletion on MDSC numbers in the spleen. Single and double depletion of $CD4^+$ and $CD8^+$ T cells in tumor-bearing mice resulted in a significant reduction of MDSC numbers (Fig. 6B). Interestingly, Mo-MDSCs were reduced to a higher extend than Gr-MDSCs (Supplementary Fig. S3A). Taken together, this experiment suggests that mainly $CD4^+$ T cells are responsible for increasing HSPC activity and myelopoiesis in tumor bearing mice. The fact that depletion of $CD4^+$ and $CD8^+$ T comparably reduced MDSCs numbers in tumor-bearing mice suggests that $CD8^+$ T cells contribute to MDSCs differentiation and accumulation by other pathways than regulating hematopoiesis in the BM.

We next analyzed if the increase in LSK numbers was mediated by a soluble factor secreted by T cells. LSKs formed more colonies in the presence of serum from MC57 tumor-bearing mice compared to serum from naive BL/6 mice. In contrast, serum from MC57 tumor-bearing $Rag^{-/-}$ mice did not increase colony formation compared to serum from naive $Rag^{-/-}$ mice (Fig. 6C). Interestingly, heat-inactivated serum from MC57 tumor-bearing mice lost its capacity to enhance colony formation (Fig. 6D), indicating that the soluble factor is a protein, most probably a cytokine that is secreted by activated T cells. To confirm our hypothesis, we performed colony assays of LSKs in the presence of conditioned media from T cell cultures (T cell-conditioned medium, TCM) originating from MC57 tumor-bearing or naive mice. $CD4^+$ TCM from MC57 tumor-bearing mice significantly increased colony formation capacity of naive LSKs, whereas $CD8^+$ TCM resulted only in a non-significant increase in colony numbers (Fig. 6E). A similar increase in colony formation was observed when adding $CD4^+$ TCM from mice bearing immunogenic 3LL tumors, but not from mice with less immunogenic MC38 tumors (Fig. 6F). Taken together, these results indicate that $CD4^+$ T cells from mice with immunogenic tumors secrete a protein that induces expansion of LSKs.

TNFα secreted by CD4$^+$ T cells increases colony formation of LSKs.

In order to define which T cell-derived factors are responsible for the observed activation of HSPCs, we performed a customized array of 48 cytokines, chemokines and growth factors (listed in methods sections) in sera and TCM of tumor-bearing or naive mice. Analysis of sera from tumor-bearing mice revealed a decreased level of 23 cytokines and an increase in 18 cytokines compared to sera from naive mice; 7 cytokines were not detected at all (Fig. 6G). In CD4$^+$ TCM, 3 cytokines were downregulated and 12 were upregulated; 33 cytokines were not detectable in TCM (Fig. 6H-I). IL-6, MIP-1α and TNFα were among the most significantly upregulated cytokines in CD4$^+$ TCMs (Fig. 6J). IL-6 is known to induce activation of hematopoiesis with a preferential myeloid differentiation during chronic inflammation (32,33). MIP-1α is known to promote myeloid differentiation through remodeling the BM niche (34). In contrast, one study indicated that MIP1α is a negative regulator of HSCs (35). TNFα has activating and inhibiting effects on HSPCs depending on its concentration and the presence of other growth factors (36).

To functionally validate whether one of the elevated cytokines is responsible for the activation of HSPCs, we analyzed colony formation of LSKs in the presence of blocking antibodies for IL-6, TNFα and MIP1α. Blocking of IL-6 and MIP1α did not reduce the elevated colony formation of LSKs in the presence of serum from tumor-bearing mice. However, blocking TNFα reduced colony formation to the level of control cultures with naive serum (Fig. 6K). In contrast, addition of TNFα increased the colony formation capacity of LKSs (Fig. 6L). Both, CD4$^+$ and CD8$^+$ T cells in spleen of tumor bearing 3LL and MC57 tumors produced TNFα (Supplementary Fig. S3B-C). Importantly, TNFα concentration in sera of mice bearing immunogenic tumors (3LL and MC57) was increased, whereas TNFα concentrations in sera of MC38 and B16F10 tumor-bearing mice was not (Fig. 6M). Furthermore, an *in silico* pathway analysis could predict that at gene/protein level, most of the elevated cytokines in sera or TCMs of tumor-bearing mice can potentially influence the expression of TNFα (Fig. 6N). Taken together, these results indicated that TNFα secreted by T cells activates HSPCs in tumor-bearing mice.

TNFα activates HSPCs and myeloid differentiation *in vivo*

In order to study the function of IL-6 and TNFα *in vivo*, we transplanted MC57 tumor fragments into IL-6$^{-/-}$ or TNFR1/2$^{-/-}$ mice. Similarly, to BL/6 mice, IL-6 deficient tumor-bearing mice had elevated numbers of LSKs and CMPs in the BM (Supplementary Fig S4A). In addition, HSPCs from tumor mice formed more colonies *in vitro* (Supplementary Fig S4B).

In line with results in other tumor models (37), transplanted MC57 tumors did only grow for up to two weeks and were then rejected in TNFR1/2$^{-/-}$ mice (Fig. 7A). Therefore, we analyzed hematopoiesis in the BM already 14 days after tumor transplantation, at a time point where tumors in BL/6 and TNFR1/2$^{-/-}$ mice were very small. Analysis of BM revealed a slight increase in LSKs and CMPs in BL/6 tumor-bearing mice compared to naive controls. In contrast, TNFR1/2$^{-/-}$ tumor-bearing mice had no increase in these cell populations (Fig. 7B-C). In addition, MDSCs in BM of tumor-bearing mice were increased in BL/6 but not in TNFR1/2$^{-/-}$ mice (Fig. 7D).

To further analyze the role of TNFα in the regulation of myelopoiesis in a second tumor model, we transplanted 3LL-Lewis lung carcinoma cells to TNFR1/2$^{-/-}$ and BL/6 mice. TNFα was significantly increased in the sera and in TCM of CD4^{+} T cells from 3LL tumor-bearing mice (Fig. 7E). Loss of function of TNFα in TNFR1/2-deficient mice normalized hematopoiesis in the BM with comparable numbers of LSKs, CMPs and GMPs in naive and tumor-bearing mice (Fig. 7F). Similarly, colony formation of Lin^{-} cells from 3LL tumor-bearing TNFR1/2$^{-/-}$ mice was comparable to naive controls (Fig. 7G). A sub-differentiation of the LSK compartment revealed that the number of the primitive HSC subsets (LT-HSC and ST-HSC) remained unchanged whereas the numbers of MPP1 and MPP2 increased significantly in 3LL tumor-bearing BL/6 mice. Importantly, MPP1 and MPP2 cell numbers in tumor-bearing TNFR1/2-/- mice were comparable to naive mice, indicating that the increase in MPP1 and 2 cells in BL/6 tumor-bearing mice is dependent on TNFα signaling. The number of MPP3, which comprises mainly lymphoid progenitors remained unchanged in BL/6 tumor-bearing mice and even dropped in TNFR1/2$^{-/-}$tumor-bearing mice (Fig. 7H). Numbers of Mo- and Gr-MDSCs in spleen were similarly reduced in TNFR1/2$^{-/-}$ tumor-bearing mice as compared to BL/6 tumor-bearing mice (Fig. 7I).

Furthermore, TNFα increased cell cycling of LSKs in tumor-bearing BL/6 mice, as indicated by a higher frequency of LSKs in S1 phase, but not in TNFR1/2$^{-/-}$ mice (Fig. 7J). Similarly, neutralization of TNFα in 3LL tumor-bearing mice by treatment with a mAb blocked the increase in LSKs, CMPs and MDSCs (Fig. 7K-M). Moreover, TNFα depletion significantly reduced tumor growth (Fig. 7N). These results confirm that TNFα increases myelopoiesis and the accumulation of MDSCs in tumor-bearing mice.

Discussion

Escape from immunosurveillance is a hallmark of cancer development (38). Thereby, tumor cells adopt strategies to overcome destruction by tumor-antigen-specific effector cells. For example, cancer cells generate an immunosuppressive microenvironment in the tumor by producing immunosuppressive factors such as PD-L1, FasL, IL-10 or TGF-β that directly inhibit the activity of anti-tumoral effector cells or by recruiting immunosuppressive cells such as Tregs and MDSCs (39). Importantly, the level of immunosuppression is a negative prognostic factor in cancer patients (4,40-43). MDSCs are one important cell population that is recruited to the tumor microenvironment and induces immunosuppression (5,7,44). Unlike lymphocytes, myeloid cells including MDSCs do not have the capacity for clonal expansion and, in addition, they have a relatively short half-life *in vivo* (45). In cancer, a high activity of reactive oxygen species (ROS) in MDSCs increases apoptosis and even reduces the life span of MDSCs (9). Thus, MDSCs need to be replenished continuously from hematopoietic precursors in the BM. Some tumor cells produce hematopoietic cytokines such as GM-CSF, G-CSF and IL-6 that increase myelopoiesis in the BM and the production of MDSCs (6-8,46). However, a majority of tumor cells does not produce hematopoietic growth factors and the mechanisms regulating hematopoiesis in these tumor types remain unknown (8). We now show that an activated adaptive immune system regulates hematopoiesis in different experimental tumor models. T cell-secreted TNFα induced emergency hematopoiesis by increasing cell cycling activity of LT- and ST-HSC and myeloid progenitors. Interestingly, analysis of HSC subsets revealed increased numbers in myeloid-skewed MPP1 and MPP2 subsets but not lymphoid-skewed MPP3s. This preferential differentiation to the myeloid lineage was confirmed by increased numbers of myeloid progenitors (CMPs and/or GMPs) with normal numbers of CLPs.

T lymphocytes control hematopoiesis through various mechanisms. In steady state, effector $CD4^+$ T cells in the BM regulate myelopoiesis and ensure terminal differentiation of myeloid cells by secreting IL-6, IL-3 and GM-CSF (47). During inflammation, cytotoxic $CD8^+$ T cells secrete IFNγ that acts on HSCs and impairs their self-renewal by dephosphorylating STAT5 (48). In addition, activated T lymphocytes

produce hematopoietic cytokines, such as colony-stimulating factors, IL-6 and IL-17 that induce myeloid differentiation and amplify granulocyte production (47). Co-culture experiments and $CD4^+$ and $CD8^+$ T cell depletion experiments revealed that the factors regulating hematopoiesis in our tumor models are mainly derived from $CD4^+$ T cells. We found that many important cytokines that are directly or indirectly involved in the regulation of the hematopoiesis such as TNFα and IL-6 are increased in the sera and in $CD4^+$ TCM from tumor-bearing mice.

We excluded a major role of $CD4^+$ T cell-secreted IL6 in the regulation of myelopoiesis *in vitro* by adding IL-6 neutralizing antibodies in colony forming assays and *in vivo* by transplanting tumors in IL-6-deficient mice. TNFα was the cytokine with the largest increase in $CD4^+$ TCM and neutralization of TNFα prevented the increase in colony forming capacity of BL/6 LSKs induced by the sera of tumor-bearing mice. Although TNFα is produced by $CD8^+$ and $CD4^+$ T cells, in vivo depletion of each cell population individually suggests that the main effect on hematopoiesis is mediated by TNFα secreted by $CD4^+$ T cells. In contrast, $CD4^+$ and $CD8^+$ T cell depletion similarly reduced MDSC numbers in tumor bearing mice, suggesting that $CD8^+$ T cell influence the differentiation to MDSCs by additional mechanisms. Importantly, transplantation of MC57 and 3LL tumors to TNFR-deficient mice indicated that TNFα leads to the activation of hematopoiesis, myeloid skewing and to the increase in MDSCs observed in tumor-bearing mice. This central role of a single cytokine in the regulation of the hematopoiesis in tumor-bearing mice was somewhat surprising, since at least 41 of the 48 cytokines studied were detected at higher or lower levels in the sera of tumor-bearing mice versus naive mice. However, an *in silico* pathway analysis suggested that TNFα interacts with and possibly regulates most of the other molecules analyzed.

TNFα signaling through its receptors (TNFR) TNFR-I (p55) and TNFR-II (p75) activates NF-κB and other signaling pathways that increases cell survival, activation and proliferation (49). The soluble form of TNFα (sTNFα) mainly triggers TNFR-I, whereas the transmembranous form (tmTNFα) preferentially activates TNFR-II (50) with distinct biological functions. It has been documented that mainly sTNFα drives the differentiation and accumulation of MDSCs in a MCA tumor model (14). The function of

TNFα in the regulation of hematopoiesis has been analyzed in different models with partially contradictory results: TNFα has been shown to suppress or increase the colony formation capacity of HSCs and their *in vivo* reconstitution capacity, probably depending on the dose and length of exposure studied (51,52). Prolonged and excessive TNFα has been associated with myelodysplastic syndromes (53). Furthermore, mice deficient of the p55 TNFR 1α (TNFRSF1α$^{-/-}$) have increased numbers of functionally impaired HSPCs as indicated by a reduced self-renewal capacity (54). Tumor development and consecutive activation of the adaptive immune system lead to a continuous production of TNFα. The transplantable tumor models have the limitation that tumors develop fast and long-term effects on hematopoiesis cannot be studied. However, the development of MCA-induced sarcoma and of lung adenocarcinoma in the KP model takes several months and therefore mimics the physiological development of a cancer and of the anti-tumoral immune response more closely. Importantly, we observed a similar increase in HSPCs with myeloid skewing independent of the growth kinetics of the tumor. Experiments using TNFR1/2$^{-/-}$ confirmed that TNFα is an important cytokine in activating myelopoiesis and, thereby, contributes to an increase in MDSC numbers. In vitro experiments with TCM suggests that the sTNFα is the main driver of the expansion of HSCs. However, TNFα not only increases MDSCs numbers by regulating HSPCs. TNFα signaling directly enhances the survival of MDSCs through cellular FLICE-inhibitory protein (c-FLIP)-mediated inhibition of caspase-8 (37) . Together, these mechanisms contribute to the tumor-resistance of TNFα-deficient mice (55).

The fact that the activated anti-tumoral immune response by itself leads to an increase in myelopoiesis and MDSCs and, thereby, to immunosuppression indicates a physiologically important regulatory system. Several comparable regulatory circuits have been described. The effector cytokine IFNγ secreted by activated T cells induces the up-regulation of the T cell inhibitory ligand PD-L1 (56). Ligation of CD27 by CD70 expressed on activated immune cells induces the expansion of Tregs and leads to an impaired tumor-immunosurveillance (57). IL-5 and IL-13 cytokines produced by T helper type 2 (Th2) cells enhance type 2 macrophage differentiation (58). Therefore, tumors escape immunosurveillance by

regulatory circuits that developed to prevent immunopathology. Defining and blocking these mechanisms led and may lead to promising therapeutic strategies to treat cancer.

Acknowledgments

This work was supported by the Swiss National Science Foundation, the Swiss Cancer League and the Werner und Hedy Berger-Janser-Stiftung,

Conflict-of-interest disclosure: The authors declare no conflict of interest.

References

1. Eaves CJ. Hematopoietic stem cells: concepts, definitions, and the new reality. Blood **2015**;125:2605-13
2. Wu WC, Sun HW, Chen HT, Liang J, Yu XJ, Wu C*, et al.* Circulating hematopoietic stem and progenitor cells are myeloid-biased in cancer patients. Proc Natl Acad Sci U S A **2014**;111:4221-6
3. Ugel S, De Sanctis F, Mandruzzato S, Bronte V. Tumor-induced myeloid deviation: when myeloid-derived suppressor cells meet tumor-associated macrophages. J Clin Invest **2015**;125:3365-76
4. Diaz-Montero CM, Salem ML, Nishimura MI, Garrett-Mayer E, Cole DJ, Montero AJ. Increased circulating myeloid-derived suppressor cells correlate with clinical cancer stage, metastatic tumor burden, and doxorubicin-cyclophosphamide chemotherapy. Cancer Immunol Immunother **2009**;58:49-59
5. Talmadge JE, Gabrilovich DI. History of myeloid-derived suppressor cells. Nat Rev Cancer **2013**;13:739-52
6. Hong IS. Stimulatory versus suppressive effects of GM-CSF on tumor progression in multiple cancer types. Exp Mol Med **2016**;48:e242
7. Casbon AJ, Reynaud D, Park C, Khuc E, Gan DD, Schepers K*, et al.* Invasive breast cancer reprograms early myeloid differentiation in the bone marrow to generate immunosuppressive neutrophils. Proc Natl Acad Sci U S A **2015**;112:E566-75
8. Steube KG, Meyer C, Drexler HG. Secretion of functional hematopoietic growth factors by human carcinoma cell lines. Int J Cancer **1998**;78:120-4
9. Condamine T, Kumar V, Ramachandran IR, Youn JI, Celis E, Finnberg N*, et al.* ER stress regulates myeloid-derived suppressor cell fate through TRAIL-R-mediated apoptosis. J Clin Invest **2014**;124:2626-39
10. Huynh H, Zheng J, Umikawa M, Silvany R, Xie XJ, Wu CJ*, et al.* Components of the hematopoietic compartments in tumor stroma and tumor-bearing mice. PLoS One **2011**;6:e18054
11. Metcalf D. The molecular control of cell division, differentiation commitment and maturation in haemopoietic cells. Nature **1989**;339:27-30
12. Dolcetti L, Peranzoni E, Ugel S, Marigo I, Fernandez Gomez A, Mesa C*, et al.* Hierarchy of immunosuppressive strength among myeloid-derived suppressor cell subsets is determined by GM-CSF. Eur J Immunol **2010**;40:22-35
13. Sade-Feldman M, Kanterman J, Ish-Shalom E, Elnekave M, Horwitz E, Baniyash M. Tumor necrosis factor-alpha blocks differentiation and enhances suppressive activity of immature myeloid cells during chronic inflammation. Immunity **2013**;38:541-54
14. Sobo-Vujanovic A, Vujanovic L, DeLeo AB, Concha-Benavente F, Ferris RL, Lin Y*, et al.* Inhibition of Soluble Tumor Necrosis Factor Prevents Chemically Induced Carcinogenesis in Mice. Cancer Immunol Res **2016**;4:441-51
15. Matter M, Pavelic V, Pinschewer DD, Mumprecht S, Eschli B, Giroglou T*, et al.* Decreased tumor surveillance after adoptive T-cell therapy. Cancer Res **2007**;67:7467-76
16. DuPage M, Dooley AL, Jacks T. Conditional mouse lung cancer models using adenoviral or lentiviral delivery of Cre recombinase. Nat Protoc **2009**;4:1064-72

17. Sharma S, Stolina M, Lin Y, Gardner B, Miller PW, Kronenberg M*, et al.* T cell-derived IL-10 promotes lung cancer growth by suppressing both T cell and APC function. J Immunol **1999**;163:5020-8
18. Cabezas-Wallscheid N, Klimmeck D, Hansson J, Lipka DB, Reyes A, Wang Q*, et al.* Identification of regulatory networks in HSCs and their immediate progeny via integrated proteome, transcriptome, and DNA Methylome analysis. Cell Stem Cell **2014**;15:507-22
19. Kim EK, Jeon I, Seo H, Park YJ, Song B, Lee KA*, et al.* Tumor-derived osteopontin suppresses antitumor immunity by promoting extramedullary myelopoiesis. Cancer Res **2014**;74:6705-16
20. Cortez-Retamozo V, Etzrodt M, Newton A, Rauch PJ, Chudnovskiy A, Berger C*, et al.* Origins of tumor-associated macrophages and neutrophils. Proc Natl Acad Sci U S A **2012**;109:2491-6
21. Bayne LJ, Beatty GL, Jhala N, Clark CE, Rhim AD, Stanger BZ*, et al.* Tumor-derived granulocyte-macrophage colony-stimulating factor regulates myeloid inflammation and T cell immunity in pancreatic cancer. Cancer Cell **2012**;21:822-35
22. Demirci U, Coskun U, Sancak B, Ozturk B, Bahar B, Benekli M*, et al.* Serum granulocyte macrophage-colony stimulating factor: a tumor marker in colorectal carcinoma? Asian Pac J Cancer Prev **2009**;10:1021-4
23. Urdinguio RG, Fernandez AF, Moncada-Pazos A, Huidobro C, Rodriguez RM, Ferrero C*, et al.* Immune-dependent and independent antitumor activity of GM-CSF aberrantly expressed by mouse and human colorectal tumors. Cancer Res **2013**;73:395-405
24. Ochsenbein AF, Klenerman P, Karrer U, Ludewig B, Pericin M, Hengartner H*, et al.* Immune surveillance against a solid tumor fails because of immunological ignorance. Proc Natl Acad Sci U S A **1999**;96:2233-8
25. Boon T. Antigenic tumor cell variants obtained with mutagens. Adv Cancer Res **1983**;39:121-51
26. LeGrue SJ, Simcik WJ, Frost P. Immunogenic variants of a murine fibrosarcoma induced by mutagenesis: requirement of viable cells for antigen-specific cross-protection. Cancer Res **1987**;47:4413-6
27. DuPage M, Mazumdar C, Schmidt LM, Cheung AF, Jacks T. Expression of tumour-specific antigens underlies cancer immunoediting. Nature **2012**;482:405-9
28. Ochsenbein AF, Sierro S, Odermatt B, Pericin M, Karrer U, Hermans J*, et al.* Roles of tumour localization, second signals and cross priming in cytotoxic T-cell induction. Nature **2001**;411:1058-64
29. Xu D, Gu P, Pan PY, Li Q, Sato AI, Chen SH. NK and CD8+ T cell-mediated eradication of poorly immunogenic B16-F10 melanoma by the combined action of IL-12 gene therapy and 4-1BB costimulation. Int J Cancer **2004**;109:499-506
30. Hodge JW, Schlom J. Comparative studies of a retrovirus versus a poxvirus vector in whole tumor-cell vaccines. Cancer Res **1999**;59:5106-11
31. Mombaerts P, Iacomini J, Johnson RS, Herrup K, Tonegawa S, Papaioannou VE. RAG-1-deficient mice have no mature B and T lymphocytes. Cell **1992**;68:869-77
32. Maeda K, Malykhin A, Teague-Weber BN, Sun XH, Farris AD, Coggeshall KM. Interleukin-6 aborts lymphopoiesis and elevates production of myeloid cells in systemic lupus erythematosus-prone B6.Sle1.Yaa animals. Blood **2009**;113:4534-40

33. Schurch CM, Riether C, Ochsenbein AF. Cytotoxic CD8+ T cells stimulate hematopoietic progenitors by promoting cytokine release from bone marrow mesenchymal stromal cells. Cell Stem Cell **2014**;14:460-72
34. Schepers K, Pietras EM, Reynaud D, Flach J, Binnewies M, Garg T*, et al.* Myeloproliferative neoplasia remodels the endosteal bone marrow niche into a self-reinforcing leukemic niche. Cell Stem Cell **2013**;13:285-99
35. Graham GJ, Wright EG, Hewick R, Wolpe SD, Wilkie NM, Donaldson D*, et al.* Identification and characterization of an inhibitor of haemopoietic stem cell proliferation. Nature **1990**;344:442-4
36. Jacobsen SE, Ruscetti FW, Dubois CM, Keller JR. Tumor necrosis factor alpha directly and indirectly regulates hematopoietic progenitor cell proliferation: role of colony-stimulating factor receptor modulation. J Exp Med **1992**;175:1759-72
37. Zhao X, Rong L, Li X, Liu X, Deng J, Wu H*, et al.* TNF signaling drives myeloid-derived suppressor cell accumulation. J Clin Invest **2012**;122:4094-104
38. Schreiber RD, Old LJ, Smyth MJ. Cancer immunoediting: integrating immunity's roles in cancer suppression and promotion. Science **2011**;331:1565-70
39. Mantovani A, Allavena P, Sica A, Balkwill F. Cancer-related inflammation. Nature **2008**;454:436-44
40. Zhang B, Wang Z, Wu L, Zhang M, Li W, Ding J*, et al.* Circulating and tumor-infiltrating myeloid-derived suppressor cells in patients with colorectal carcinoma. PLoS One **2013**;8:e57114
41. Chi N, Tan Z, Ma K, Bao L, Yun Z. Increased circulating myeloid-derived suppressor cells correlate with cancer stages, interleukin-8 and -6 in prostate cancer. Int J Clin Exp Med **2014**;7:3181-92
42. Eruslanov E, Neuberger M, Daurkin I, Perrin GQ, Algood C, Dahm P*, et al.* Circulating and tumor-infiltrating myeloid cell subsets in patients with bladder cancer. Int J Cancer **2012**;130:1109-19
43. Gabitass RF, Annels NE, Stocken DD, Pandha HA, Middleton GW. Elevated myeloid-derived suppressor cells in pancreatic, esophageal and gastric cancer are an independent prognostic factor and are associated with significant elevation of the Th2 cytokine interleukin-13. Cancer Immunol Immunother **2011**;60:1419-30
44. Khaled YS, Ammori BJ, Elkord E. Myeloid-derived suppressor cells in cancer: recent progress and prospects. Immunol Cell Biol **2013**;91:493-502
45. Summers C, Rankin SM, Condliffe AM, Singh N, Peters AM, Chilvers ER. Neutrophil kinetics in health and disease. Trends Immunol **2010**;31:318-24
46. Bronte V, Chappell DB, Apolloni E, Cabrelle A, Wang M, Hwu P*, et al.* Unopposed production of granulocyte-macrophage colony-stimulating factor by tumors inhibits CD8+ T cell responses by dysregulating antigen-presenting cell maturation. J Immunol **1999**;162:5728-37
47. Monteiro JP, Benjamin A, Costa ES, Barcinski MA, Bonomo A. Normal hematopoiesis is maintained by activated bone marrow CD4+ T cells. Blood **2005**;105:1484-91
48. de Bruin AM, Demirel O, Hooibrink B, Brandts CH, Nolte MA. Interferon-gamma impairs proliferation of hematopoietic stem cells in mice. Blood **2013**;121:3578-85

49. Sedger LM, McDermott MF. TNF and TNF-receptors: From mediators of cell death and inflammation to therapeutic giants - past, present and future. Cytokine Growth Factor Rev **2014**;25:453-72
50. Brenner D, Blaser H, Mak TW. Regulation of tumour necrosis factor signalling: live or let die. Nat Rev Immunol **2015**;15:362-74
51. Backx B, Broeders L, Bot FJ, Lowenberg B. Positive and negative effects of tumor necrosis factor on colony growth from highly purified normal marrow progenitors. Leukemia **1991**;5:66-70
52. Bryder D, Ramsfjell V, Dybedal I, Theilgaard-Monch K, Hogerkorp CM, Adolfsson J*, et al.* Self-renewal of multipotent long-term repopulating hematopoietic stem cells is negatively regulated by Fas and tumor necrosis factor receptor activation. J Exp Med **2001**;194:941-52
53. Gersuk GM, Beckham C, Loken MR, Kiener P, Anderson JE, Farrand A*, et al.* A role for tumour necrosis factor-alpha, Fas and Fas-Ligand in marrow failure associated with myelodysplastic syndrome. Br J Haematol **1998**;103:176-88
54. Rebel VI, Hartnett S, Hill GR, Lazo-Kallanian SB, Ferrara JL, Sieff CA. Essential role for the p55 tumor necrosis factor receptor in regulating hematopoiesis at a stem cell level. J Exp Med **1999**;190:1493-504
55. Popivanova BK, Kitamura K, Wu Y, Kondo T, Kagaya T, Kaneko S*, et al.* Blocking TNF-alpha in mice reduces colorectal carcinogenesis associated with chronic colitis. J Clin Invest **2008**;118:560-70
56. Abiko K, Matsumura N, Hamanishi J, Horikawa N, Murakami R, Yamaguchi K*, et al.* IFN-gamma from lymphocytes induces PD-L1 expression and promotes progression of ovarian cancer. Br J Cancer **2015**;112:1501-9
57. Claus C, Riether C, Schurch C, Matter MS, Hilmenyuk T, Ochsenbein AF. CD27 Signaling Increases the Frequency of Regulatory T Cells and Promotes Tumor Growth. Cancer Res **2012**;72:3664-76
58. Martinez FO, Gordon S. The M1 and M2 paradigm of macrophage activation: time for reassessment. F1000Prime Rep **2014**;6:13

Figure Legends

Figure 1: Increased myelopoiesis in MC57 fibrosarcoma-bearing mice. (A-E) MC57 cells were injected s.c. into the flanks of $Rag^{-/-}$ mice. Two weeks later, tumors were fragmented and 2 mm^3 pieces were transplanted s.c. into the flanks of BL/6 mice. Tumor-bearing mice were sacrificed 4 weeks after tumor transplantation and BM, blood and spleen were analyzed. **(A)** Frequency of T cells, B cells and myeloid cells in spleen. **(B)** $CD11b^+$ $Gr1^+$ MDSC numbers in spleen and BM. **(C)** Ratio of T cells to MDSCs in spleen and BM. Data in (A-C) are representative of three independent experiments, (n=5-10 mice/group). **(D)** Correlation of tumor size with the number of MDSCs in spleen, BM and tumor (n=5-9 mice) **(E)** [^{3}H]-Thymidine incorporation of αCD3ε-activated T cells in the presence of MDSC from naive or tumor-bearing mice in duplicates. Data are representative of 2 independent experiments, (n=4 mice/ group). Data is shown as mean±SEM. Statistics: Student's *t*-test (A-E)

Figure 2: HSPCs are activated in BM of tumor-bearing mice. (A-C) FACS analysis of BM in tumor-bearing or naive BL/6 mice 30 days after MC57 tumor transplantation. **(A)** Numbers of Lin^- HSPCs. **(B)** Numbers of LSKs, CMPs and GMPs. **(C)** Numbers of CLPs. Data in (A-C) are representative of three independent experiments, (n=9-11 mice/group) **(D)** Colony formation of FACS-sorted Lin^- cells, LSKs or CMPs from BM of tumor-bearing or naive mice. Data are representative 3 independent experiments, (n=5 mice/group). **(E-F)** FACS analysis of LSK subpopulations in BM. LT-HSC: long-term HSC, ST-HSC: short-term HSC, MPP: multipotent progenitors. Data are representative of 3 independent experiments, (n=5-10 mice/group). **(G)** Numbers of Lin^- cells in spleen and blood (ul of plated blood) of naive or tumor-bearing mice determined by FACS. **(H)** Colony formation of splenocytes or blood cells. Number of colonies per spleen or ul of plated blood are shown respectively. Data in (G-H) are representative of two independent experiments, (n=4-11 mice/group). **(I)** Representative FACS plots showing Lin^-CD45^+ LSKs MACS-purified $CD45^+$ TILs. **(J)** BM transplantation of FACS-sorted LSKs isolated from tumors or from BM cells of naive BL/6 mice, into lethally irradiated Ly5.1 recipient mice. Percentage of donor cells at week 18 after BM transplantation is shown. Data in (I-J) are representative of two independent experiments, (n= 3-5 mice/group). Data are shown as mean±SEM. Statistics: Student's *t*-test (A-H)

Figure 3: Activation of HSPCs in tumor mice and reconstitution in secondary recipients. (A) Frequency of cell cycle phases analyzed by DAPI staining of FACS-sorted LSKs from naive or tumor-bearing mice. Data are representative of three independent experiments, (n=5-10 mice/group). **(B)** Frequency of $BrdU^+$ cells *in vivo* in naive or tumor-bearing mice after 2 days of BrdU incorporation at day 28 after tumor transplantation. Data are representative of 2 independent experiments, (n=4-5 mice/group). **(C)** Frequency of Annexin-V^+ (Annex-V^+) LSKs 28 days after tumor transplantation. Data are representative of 2 independent experiments, (n=3 mice/group). **(D)** BM cells (10^5 cells) from tumor-bearing (day30) or naive Ly5.2 BL/6 mice were transplanted into lethally irradiated Ly5.1 recipient mice together with rescue BM cells ($2x10^5$ cells). **(E-F)** Percent of $Ly5.2^+$ donor cells (E) and LSKs (F) in BM of $Ly5.1^+$ recipient mice at week 18 after BM transplantation. Data in (D-F) are representative of two independent experiments, (n=4 mice/group). Data are shown as mean±SEM. Statistics: 1-way ANOVA (A), Student's *t*-test (B-C, E-F).

Figure 4: Myelopoiesis in different tumor models. **(A-F)** Tumor fragments were transplanted s.c. into BL/6 mice. BM of tumor-bearing or naive mice were analyzed 3-4 weeks after transplantation and colony formation of Lin^- cells from BM was assessed. **(A-B)** MC38 colon carcinoma. **(C-D)** B16F10 melanoma. **(E-F)** 3LL Lewis Lung carcinoma. Data in **(A-F)** are representative of three independent experiments, (n=5 mice/group). **(G-H)** MCA-induced sarcoma. 250 μg MCA, dissolved in oil, or oil alone was injected s.c. into BL/6 mice. BM was analyzed 3 months later. **(G)** LSKs in BM. **(H)** Colony formation of Lin^- cells from BM. Data in **(G-H)** are representative of two independent experiments, (n=5-7 mice/group). **(I-J)** BM analysis of lung tumor KP (K-$ras^{LSL\text{-}G12D/WT}$; $p53^{Fl/Fl}$) mice or littermate control mice 5 weeks after tumor induction. **(I)** LSKs in BM. **(J)** Colony formation of Lin- cells from BM of tumor-bearing mice or littermate controls. Data in (I-J) are representative of 2 pooled experiments, (n=4-6 mice/group). Data are shown as mean±SEM. Statistics: Student's *t*-test (A-J).

Figure 5: The adaptive immune system activates HSPCs in tumor-bearing mice. (A) Colony formation of LSKs from BL/6 naive mice, in the presence of conditioned media (CM) from the tumor cell lines MC57, B16F10, MC38 and 3LL or recombinant GM-CSF (25 ng/ml). Colonies with medium only served as controls. Data are representative of two independent experiments. **(B)** GM-CSF concentration in supernatants of tumor cell lines after 3 days of culture or sera from naive or MC57-tumor-bearing BL/6 mice 30 days after tumor transplantation run in triplicates were analyzed by cytometric bead analysis. **(C)** MC57 tumor fragments were transplanted s.c. into $Rag^{-/-}$ mice. Numbers of HSPCs in BM 3 weeks after tumor transplantation. **(D)** Colony formation of Lin^- BM cells of tumor-bearing or naive $Rag^{-/-}$ mice. Data are representative of 3 independent experiments, (n=8-15 mice/group). **(E)** Fold change of $CD11b^+$ $Gr1^+$ MDSC numbers in spleens of BL/6 or $Rag^{-/-}$ tumor-bearing mice compared to naive counterparts. Data are representative of three independent experiments (n=5 mice/group). Data are shown as mean±SEM. Statistics: Student's *t*-test (A-E).

Figure 6: A protein secreted by T cells activates HSPCs. **(A-B)** MC57 tumor-bearing or naive BL/6 mice were treated with 100 μg depleting anti-CD4-, anti-CD8- or both antibodies at days -1, 0, 7, 14 and 28 after tumor transplantation. Control mice were treated with rat IgG. Three weeks after tumor transplantation, BM and spleen were analyzed. **(A)** Fold change of LSK (left) and CMP (right) numbers in BM of tumor-bearing mice compared to naive mice. **(B)** Fold change of Gr-MDSC (left) and Mo-MDSC (right) counts in spleen of tumor-bearing mice compared to naive controls. Data shown in (A-B) are pooled from four independent experiments, (n=3-8 mice/group). **(C-E)** FACS-sorted LSKs from naive BL/6 mice were cultured in methylcellulose in the presence of indicated sera or TCM. **(C)** Increase (%) in colony formation of LSKs treated with MC57 tumor vs. naive sera (100%). **(D)** Colony formation of LSKs in the presence of heat-inactivated serum from naive or MC57 tumor-bearing BL/6 mice. **(E)** Colony formation of LSKs in the presence TCMs from naive or MC57 tumor-bearing BL/6 mice. Data in **(C-E)** are representative of two independent experiments, (n=3 mice/group). (F) Colony formation of LSKs in the presence of $CD4^+$ TCM from naïve or 3LL/MC38 tumor-bearing BL/6 mice (n=3 mice/group) **(G-N)** Analysis of cytokine secretion profile of T cells in tumor-bearing mice. **(G-J)** Sera and $CD4^+$ TCM from tumor-bearing 28 days after transplantation or naive BL/6 mice were analyzed for cytokines, chemokines and growth factors by cytokine bead assay (complete list in methods section). **(G-H)** Heat maps of relative cytokine concentrations in sera (tumor-bearing vs. naive mice **(G)**) and $CD4^+$ TCM (tumor-bearing vs. naive mice **(H)**). **(I)** Histogram indicating log2 fold change of the indicated soluble factors in $CD4^+$ TCM from tumor-bearing vs. naive mice. **(J)** Volcano plot of p-value versus the mean of fold change for the indicated soluble factors in $CD4^+$ TCM from tumor-bearing (CD4-T TCM) versus naive mice (CD4-N TCM). Data in **(G-J)** are representative of duplicates of sera or TCM pooled from 5 mice in each condition. **(K)** Colony formation of naïve FACS-sorted LSKs from naive BL/6 mice in the presence of 5 μg/ml of the indicated blocking antibodies together with serum from naive or tumor-bearing mice run in triplicates. Data are representative of two independent experiments. **(L)** LSK colony formation in the presence of titrated concentrations of TNFα. **(M)** TNFα concentration in sera of naïve, MC57, 3LL, MC38 and B16F10 tumor-bearing mice (n=4-12 mice/group). Pooled data from three

independent experiments. **(N)** *In silico* pathways analysis of TNFα interaction with the indicated cytokines. Data are shown as mean±SEM. Statistics: 1-way Anova **(A, B, I, J)**, Student's *t*-test **(C-E).**

Figure 7: Activation of HSPCs and myelopoiesis in MC57 and 3-LL-Lewis lung carcinoma tumor-bearing mice is TNFα dependent. (**A-D**) MC57 tumor fragments were transplanted s.c. into the flanks of TNFR1/2$^{-/-}$ or BL/6 mice. **(A)** Tumor size at indicated time points after transplantation in TNFR1/2$^{-/-}$ mice. **(B-C)** Numbers of LSKs and CMPs in BM 14 days after tumor transplantation. **(D)** Numbers of MDSCs in BM 14 days after transplantation. Data in (**A-D**) are representative of 3 independent experiments, (n=3 mice/group). **(E-J)** 3LL tumor fragments were transplanted into BL/6 or TNFR1/2$^{-/-}$ mice. 15 days later, sera, BM and spleen were analyzed. **(E)** Fold change of the concentration of TNFα in sera (S) or CD4^{+} TCM of tumor vs. naive BL/6 mice. Data are representative of duplicates of pooled sera or TCM from 3 mice in each condition. **(F)** HSPC counts in BM. **(G)** Colony formation of Lin^{-} cells from BM. **(H)** Numbers of HSC subpopulations in BM. **(I)** MDSC counts in spleen. Gr: granulocytic, Mo: monocytic. **(J)** FACS-sorted LSKs were stained with DAPI and the percentage of cells in S-phase is shown. Data in (**E-J**) are representative of 3 independent experiments, (n=3-5 mice/group). **(K-N)** 3LL tumor fragments were transplanted into BL/6 mice and mice were injected twice per week with anti-TNFα or IgG. **(K-M)** Absolut number and fold change of LSKs (K) and CMPs (L) between naïve and tumor-bearing mice after IgG or anti-TNFα treatment. **(M)** MDSCs per spleen in naïve and 3LL tumor-bearing mice after IgG or anti-TNFα treatment. **(N)** Tumor growth curve. **(L-N)** BM and spleen were analyzed by FACS 3 weeks after tumor transplantation (n=5 mice/group). Data are shown as mean±SEM. Statistics: Student's *t*-test (A-N) and Two-way Anova (N).

Figure 1

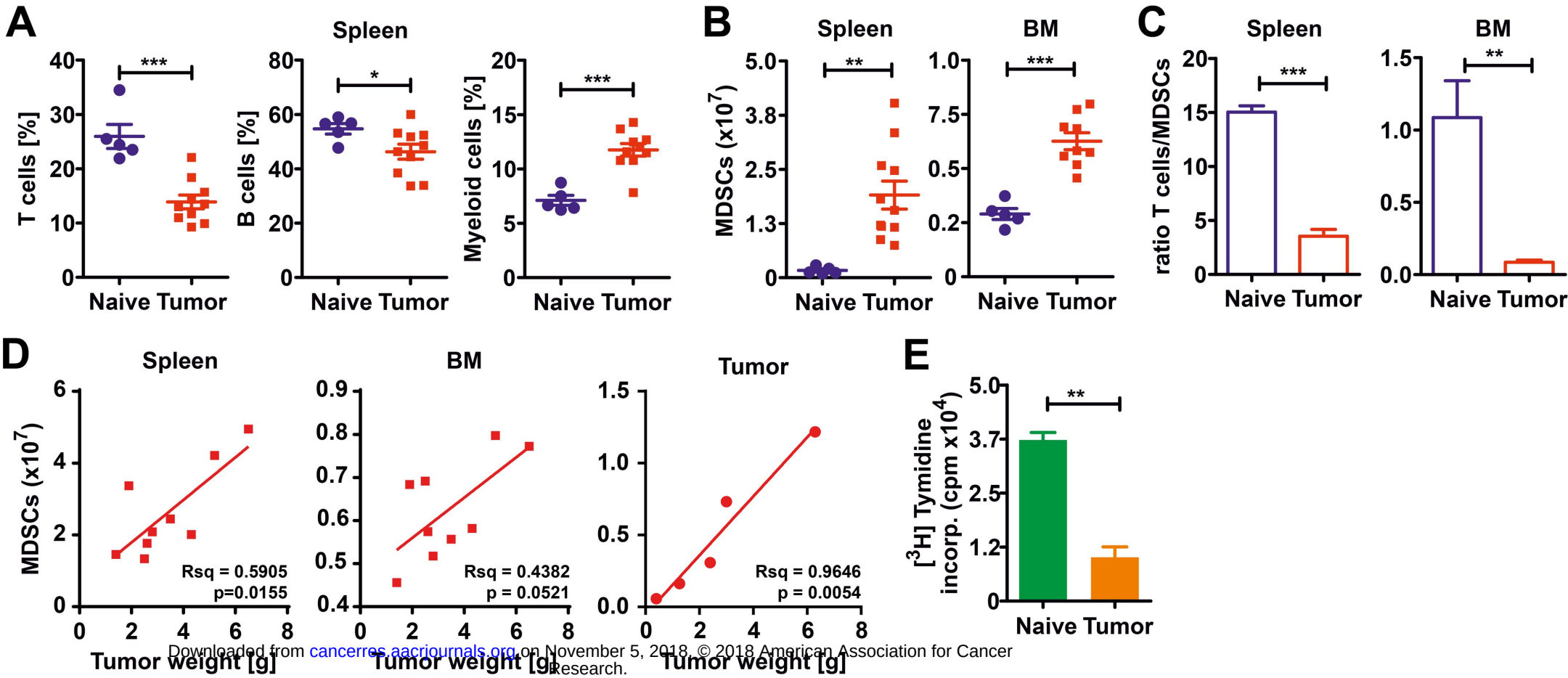

Figure 2

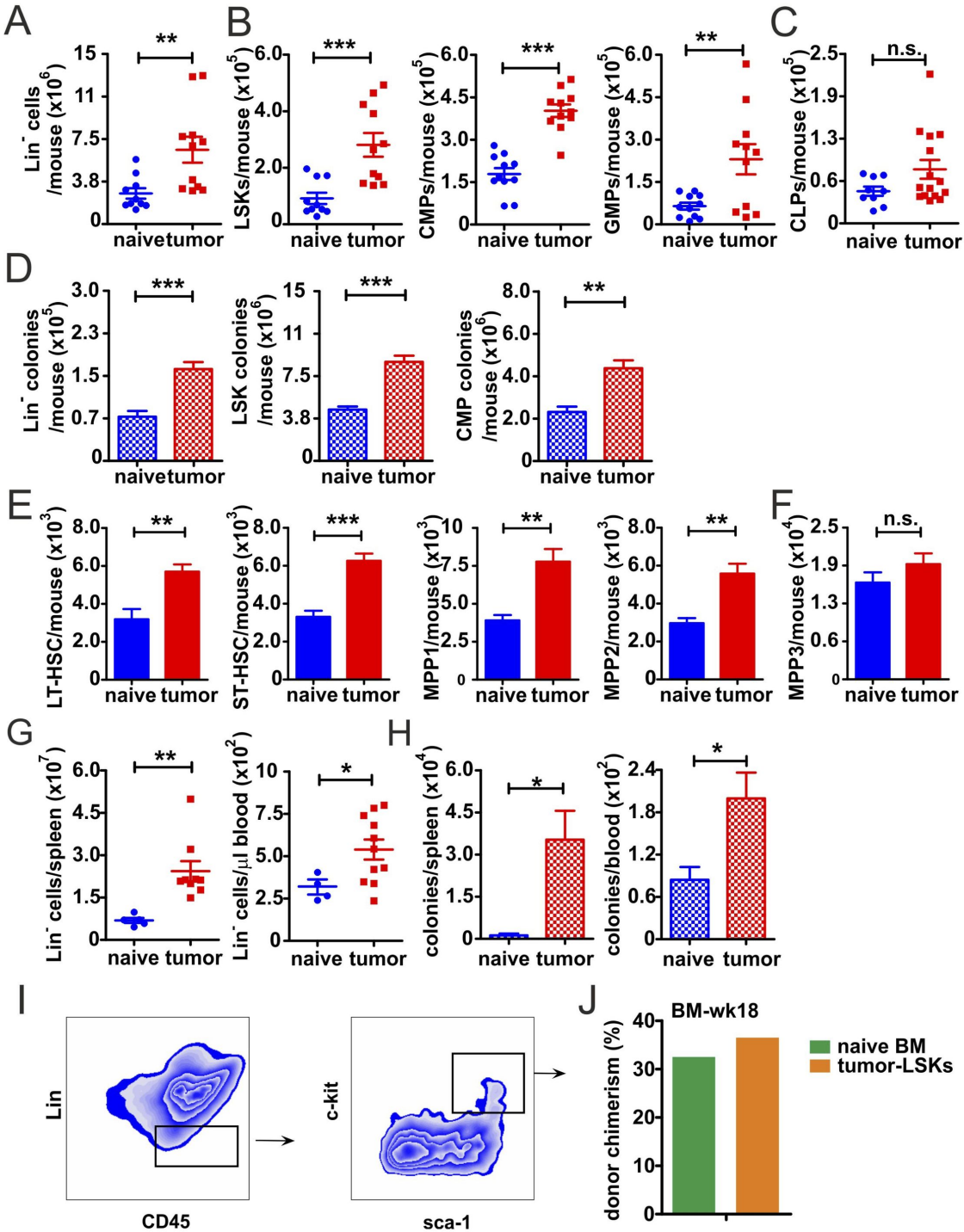

Figure 3

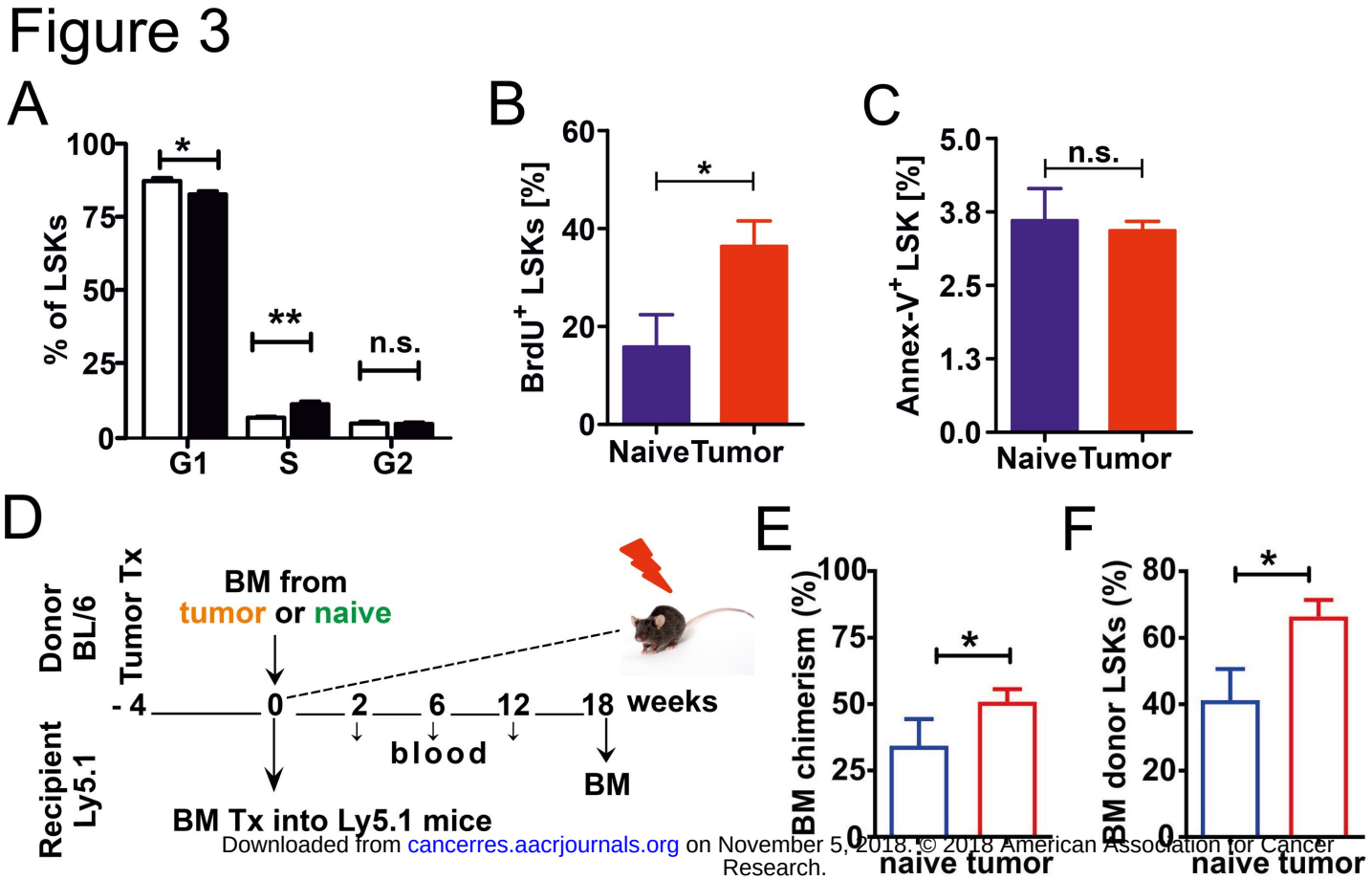

Figure 4

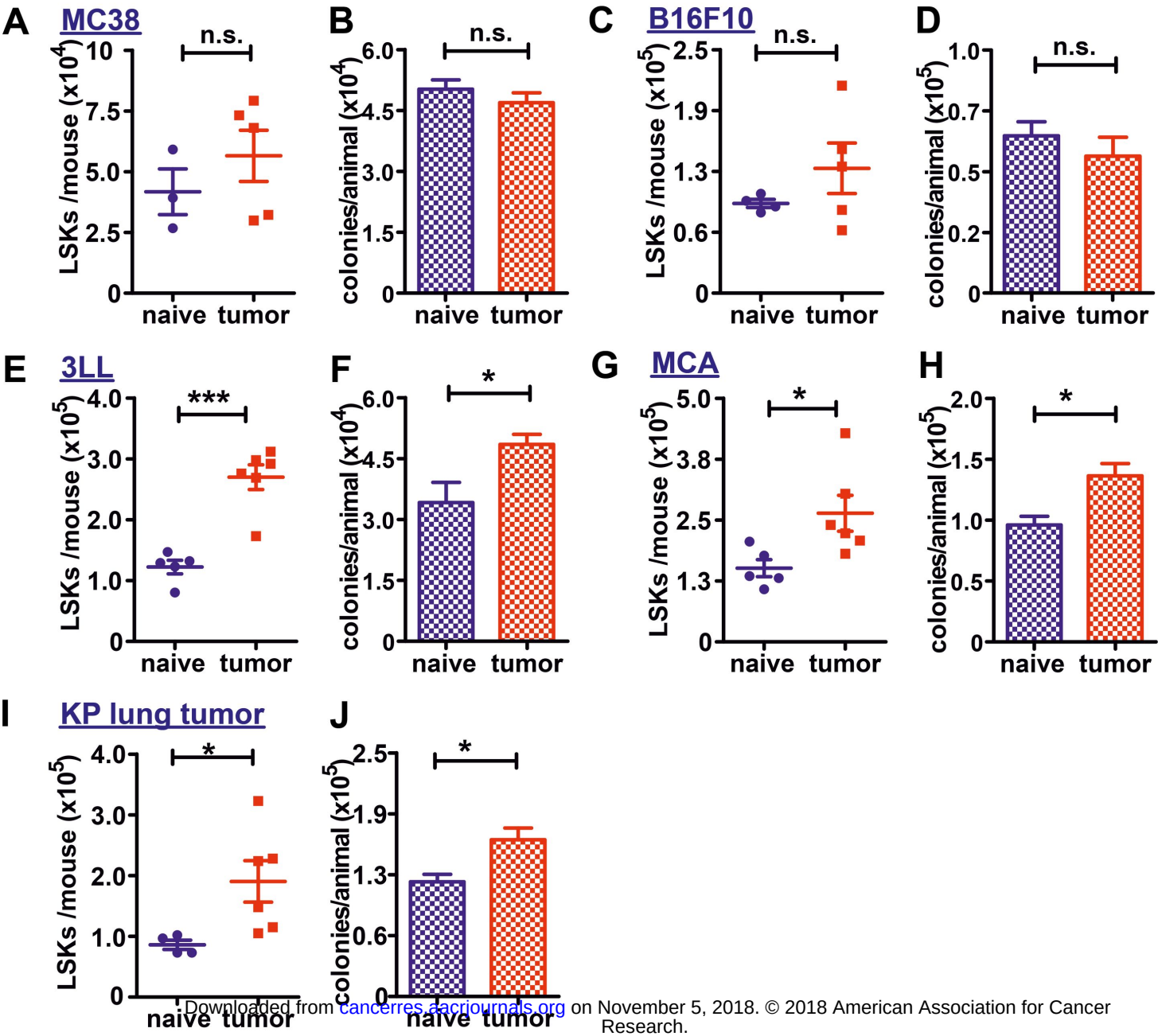

Figure 5

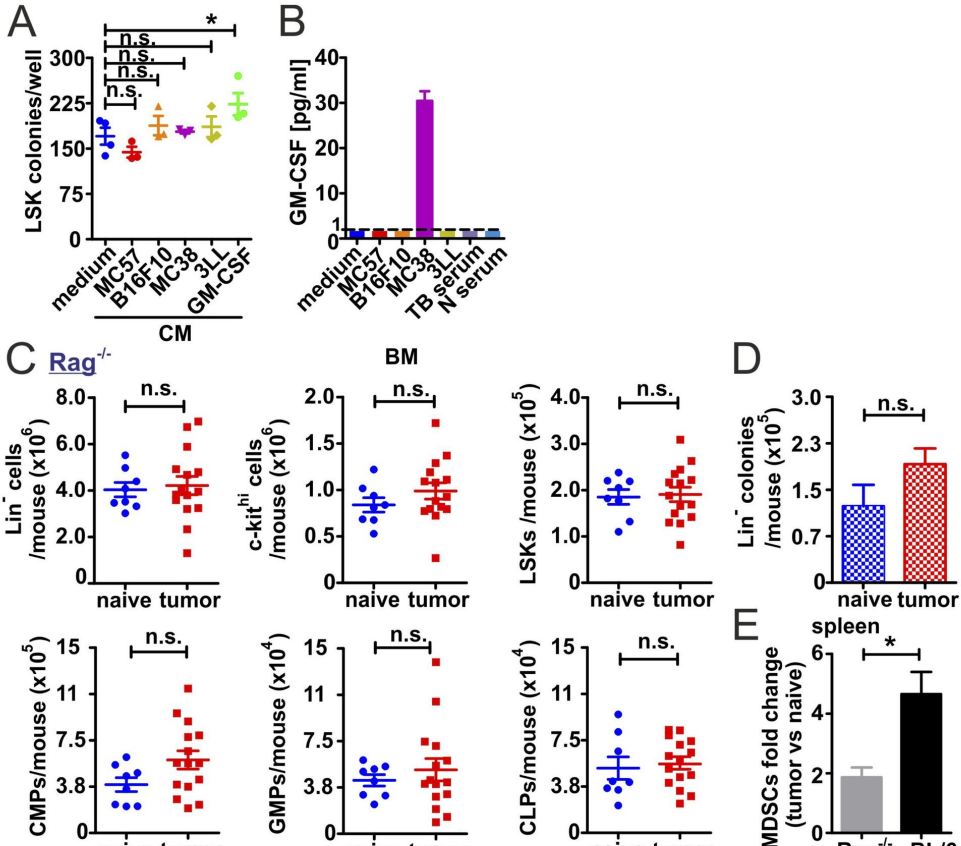

Figure 6

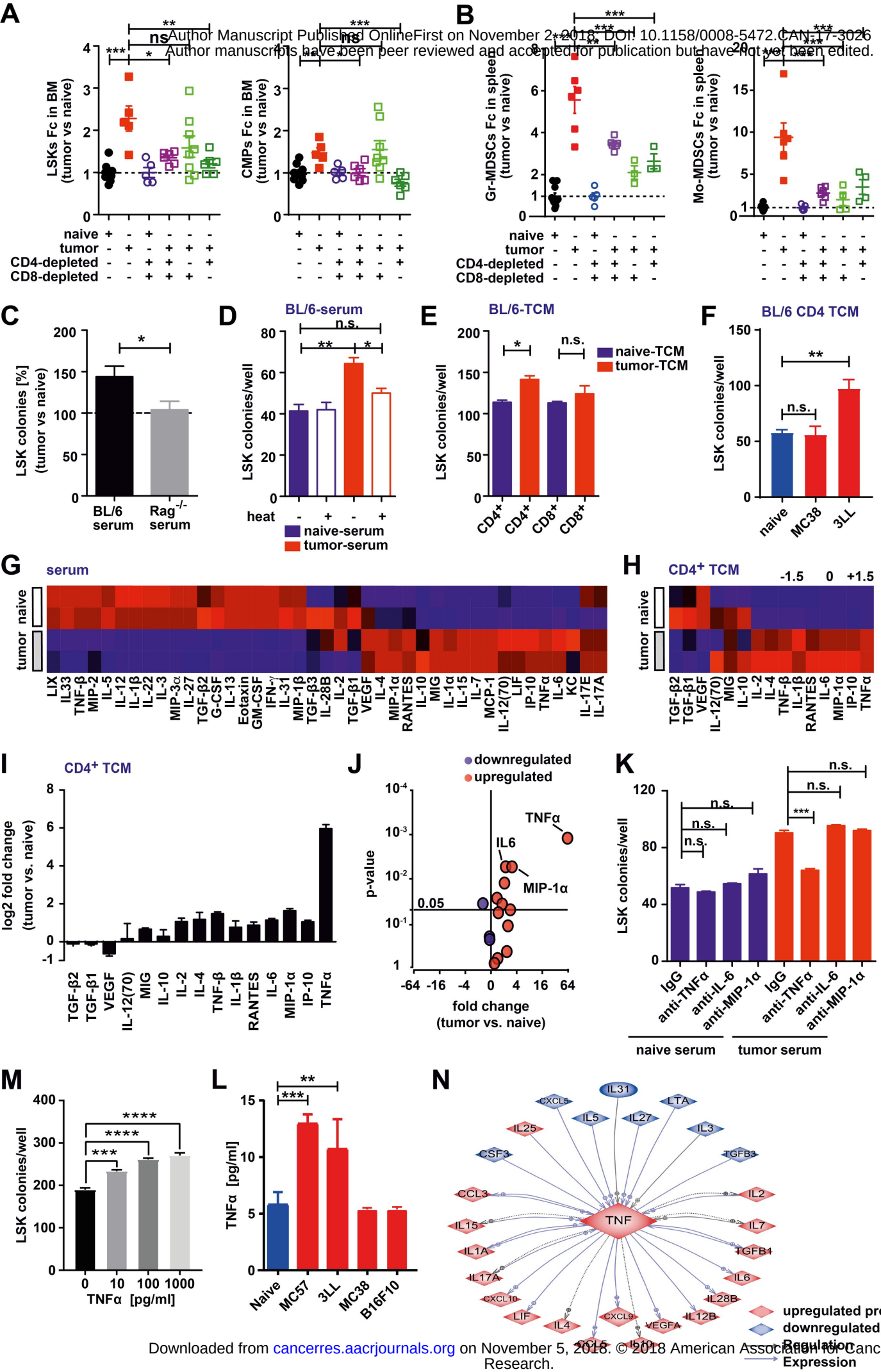

Figure 7

Cancer Research
The Journal of Cancer Research (1916–1930) | The American Journal of Cancer (1931–1940)

AACR American Association for Cancer Research

T-cell-secreted TNF-alpha induces emergency myelopoiesis and myeloid-derived suppressor cell-differentiation in cancer

Mohamad F Al Sayed, Michael Alex Amrein, Elias D. Bührer, et al.

Cancer Res Published OnlineFirst November 2, 2018.